Proceedings of the 21st ICSMGE, Vienna, Austria, 14 – 19 June 2026. Pistrol, Adam & Schweiger (eds.)
Published by: ÖGG, Austrian Society for Geomechanics, Salzburg, Austria, ISBN 978-3-9503898-4-5
https://doi.org/10.53243/ICSMGE2026-431

Seismic soil–tunnel–building interaction during high frequency earthquakes.

[1*]Juan Manuel Mayoral, [1]Simón Tepalcapa, [1]Mauricio Pérez, and [2]Azucena Román-de la Sancha
*[1]Institute of Engineering, National Autonomous University of Mexico, Mexico, *jmayoralv@iingen.unam.mx*
[2]Tecnólogico de Monterrey, School of Engineering and Science, Mexico

ABSTRACT: It is well established that tunnel-soil-building interaction effects can modified the frequency content and spectra accelerations expected to occur in free field for both interface and intraplate events. However, to date, there is a lack of information regarding tunnel-soil-building interaction for local high frequency earthquake. This effect is exacerbated in densely populated urban areas, such as Mexico City, where interaction effects among adjacent structures such as underground infrastructure, buildings and bridges can also play a significant role in the modification of the incoming seismic waves. Seeking to study the seismic soil–tunnel–building interaction during local earthquakes, a 5-story masonry building located near a metro station currently under construction was selected as a test site for seismic instrumentation. The site is found in Mexico City, in the so-called hill zone, where cemented sandy silt and silty sands can be found. This site is about 1 to 2 km away from several local faults that have exhibited high activity recently. An arrangement of four accelerometers was deployed at the site, to assess the free-field, near-field, and building seismic response. This paper presents the results gathered from the seismic instrumentation after recording eight local earthquakes. For the earthquakes recorded, it is clearly noticed that the presence of the tunnel increases the seismic response expected to occur in the tunnel vicinity, affecting nearby structures.

KEYWORDS: Soil–tunnel–building interaction, local earthquakes, seismic instrumentation, risk, underground infrastructure.

1 INTRODUCTION

Several researchers have established the impact that underground infrastructure have on the seismic response of the free field soil, and nearby buildings (e.g. Baziar et al. 2014; Pitilakis et al. 2014; Hashash et al., 2018, Mayoral et al., 2023, 2025; Mayoral & Mosqueda, 2020). Based on the results gathered from shaking table tests, Moghadam and Baziar (2016) reported an attenuation of the seismic response at the surface due to the presence of the tunnel. On the other hand, the results obtained by Wang et al, 2018, also through shaking table tests, suggest that the presence of the tunnel amplifies the surface response. In most recent studies, Mayoral and Mosqueda (2021), demonstrated through a numerical study that interaction can be beneficial or detrimental, depending on the characteristics of the seismic movement. Likewise, Mayoral et al. (2023) established, through an instrumented case study, that the effect of the seismic interaction among the soil, tunnel, and building depend largely on the type of seismic event (i.e., the seismogenic source and its magnitude), concluding that even in low- to medium-magnitude events, the presence of the tunnel leads to: amplification of the maximum ground acceleration, PGA, incoherent ground motions, and amplification of spectral accelerations, Sa, at high frequencies. Given these findings, the issue becomes critical in densely populated urban areas, where on-ground and underground infrastructure interaction during sustained and seismic loading is becoming more common to occur within their economic life. Therefore, it is important to study the seismic interaction between surface and underground structures considering all sources of seismic risk. This paper presents the data gathered from seismic instrumentation in a soil-tunnel-building system after recording eight local earthquakes at a site in Mexico City, and the main findings regarding the observed interaction effects.

2 SEISMIC ENVIRONMENT

The seismic risk in Mexico City is mostly controlled by: (1) Interface events that occur along the Pacific Coast due to the subduction of the Cocos plate under the North American Plate at depths between 5 and 40 km (Zuñiga and Suarez, 2017). An example of this type of event is the M8.1 1985 Michoacan earthquake; (2) Intraplate events, which can occur far from the Pacific Coast, within the continental crust. These events occur when the oceanic plate (i.e., the Cocos Plate) ruptures at depths of between 40 and 460 km (e.g. M7.1 2017 Puebla earthquake); (3) Cortical earthquakes, associated to the volcanic activity in the trans-volcanic north American belt; and 4) Local earthquakes, which are originated in faults found within the city, so they are strongly related to the formation of mountain chains surrounding Mexico City. According to Jaimes and Suárez (2025), the magnitude that can reach these types of earthquakes correspond to M 5.5, nevertheless their main characteristic is that their energy is concentrated in high frequencies (>10 Hz).

3 CASE STUDY

The case study corresponds to a 5-story masonry building located 2.5 m away from a tunnel, with a 10.5 m soil cover (Figure 1). Figure 2 shows a schematic representation of the case study. The instrumented site is found in the northwestern region of Mexico City. The tunnel runs through the so-called hill zone. The tunnel geometry is a standard horseshoe cross section with an external width of 17.0 m.

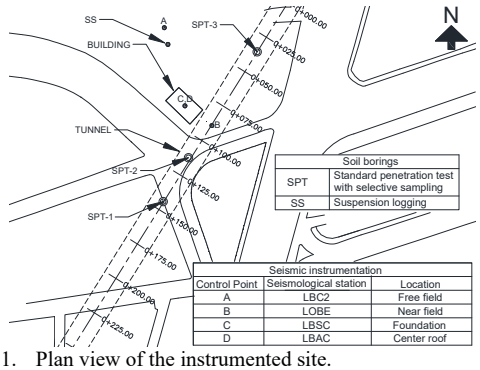

Figure 1. Plan view of the instrumented site.

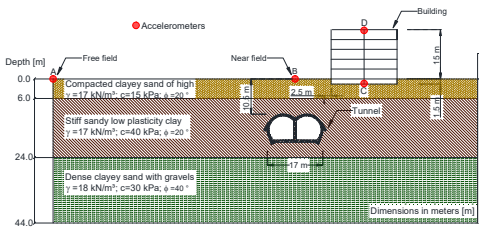

Figure 2. Schematic representation of the case study.

3.1 *Seismic instrumentation*

Seeking to study the seismic soil–tunnel–building interaction, an arrangement of four accelerometers were deployed at four key locations: free field (control point A), near field (control point B), building foundation (control point C), and building roof (control point D).

This paper presents the results gathered from the seismic instrumentation after recording eight local earthquakes. The characteristics of each earthquake are described in Table 1.

Table 1. Recorded local earthquakes.

Earthquake name	Date	Magnitude (Mw)	Depth (km)	Epicentral distance (km)
Miguel H 1	07/10/2024	2	1	2
Oztotepec	11/10/2024	2.4	7.5	28
Xochimilco	14/10/2024	2.2	1	17
Ajusco 1	15/10/2024	2.2	6	19
Coyoacán	20/10/2024	1.5	1	5
Ajusco 2	21/10/2024	1.5	7	19
Ajusco 3	21/10/2024	1.7	7	19
Miguel H 2	23/10/2024	1.4	0.8	5

4 EFFECT OF THE TUNNEL ON THE FREE FIELD RESPONSE

Figures 3, 4 and 5 summarize the peak ground acceleration, PGA, recorded at the near field and free field for all ground motion components. As described before, the tunnel changes the amplitude of the free field ground motions. The amplification factor due to the tunnel, AF_t, defined as the ratio between the PGA at the near field and free field, PGA_{nf}/PGA_{ff}, ranges from 0.68 to 4.39 and has an average value of 2.07. The lowest ground motion amplification occurred for the Oztotepec earthquake, which can be associated with the fact that it is the most distant of the reported events. This event also exhibited a slight PGA attenuation for N00W and vertical components, as in the case of Xochimilco for the vertical component. However, the remaining 88% of the records present a PGA amplification, associated with the interaction effect with the tunnel.

Figures 6, 7 and 8 depicts the comparison of the response spectra obtained for the stations in the free field (without the effect of the tunnel, control point A) and the near field (with the effect of the tunnel, control point B), which are normalized by the PGA. The response spectrum shows that the presence of the tunnel slightly modifies the frequency content, and the maximum spectral acceleration moves towards the higher frequency ranges (i.e. shorter periods). This modification is greater for the vertical component, and smaller for the remaining two.

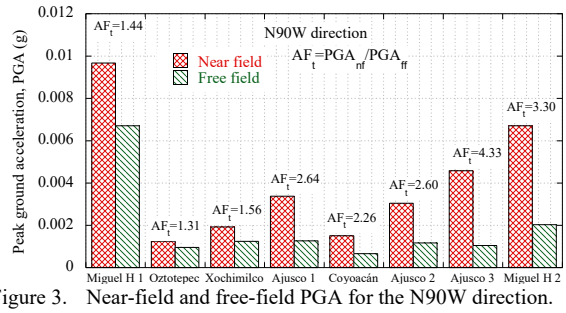

Figure 3. Near-field and free-field PGA for the N90W direction.

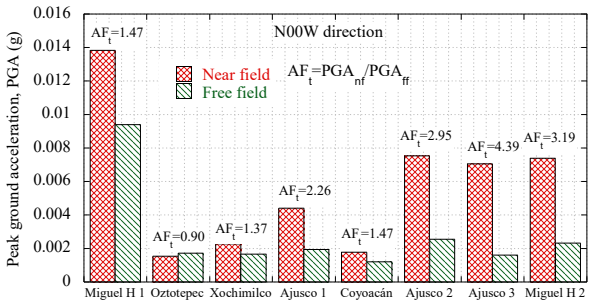

Figure 4. Near-field and free-field PGA for the N00W direction.

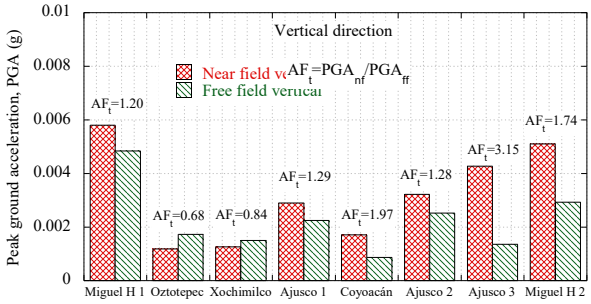

Figure 5. Near-field and free-field PGA for the Vertical direction.

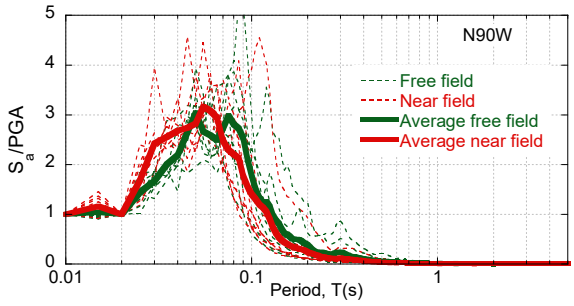

Figure 6. Normalized response spectra for the N90W component.

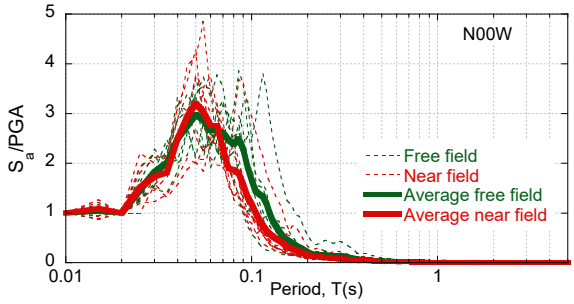

Figure 7. Normalized response spectra for the N00W component.

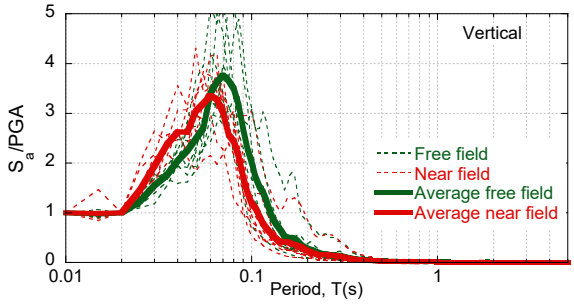

Figure 8. Normalized response spectra for the vertical component.

As has been reported for other types of seismic events, the effect of the tunnel is more important at high frequencies (Mayoral et al 2023) at the studied site. Figure 9 presents the Fourier spectra of the different types of earthquakes recorded at the study site,

including one of the local earthquakes. This figure also shows the fundamental frequency of the ground and the corresponding to the four principal vibration modes. The fundamental frequency, f_0=2.77Hz (To= 0.36s), was calculated from the shear wave velocity measured at the site using the suspension logging technique (Figure 10) and corroborated through HSVR spectral relationship analysis.

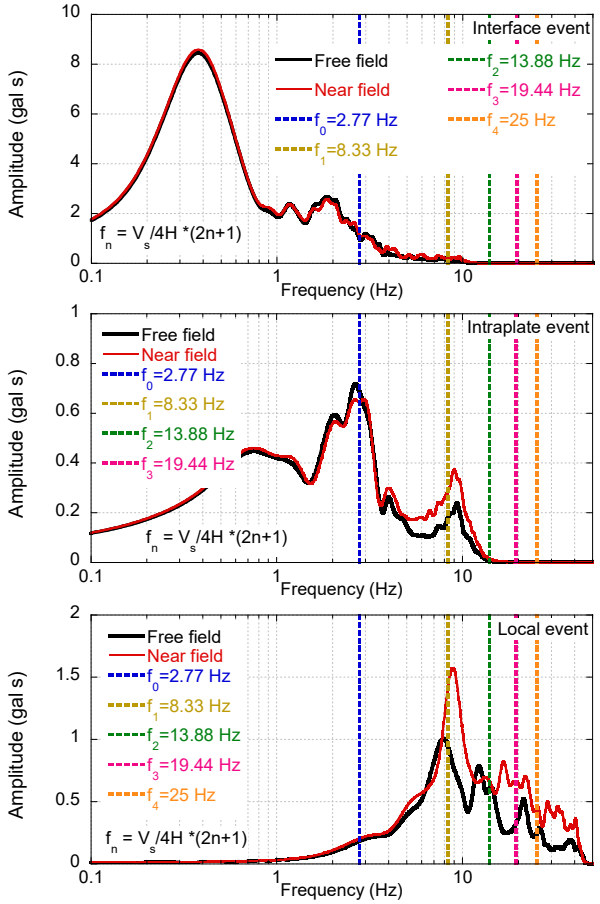

Figure 9. Fourier spectra of earthquakes from different seismogenic sources recorded at the study site.

Due to interface events concentrate their energy at low frequencies, the tunnel effect is negligible. On the other hand, intraplate events concentrate their energy at higher frequencies than interface events, so the tunnel effect increases. As can be seen for the intraplate event, the presence of the tunnel decreases the amplitude of the movement for frequencies close to 2.70 Hz, perhaps associated with the kinematic interaction between the tunnel and the surrounding soil at f_0=2.77Hz, while they increase from 3.5 Hz. Likewise, an amplification peak is observed for frequencies close to the second fundamental period f_1=8.33 Hz. Interestingly now the near field response is larger than the free field response.

Local events are characterized by concentrating their energy at higher frequencies than intraplate earthquakes. As can be observed, there is an increase in the amplitude of the movement for frequencies greater than 4 Hz, and it reaches its maximum amplitude for frequencies close to f_1=8.33 Hz.

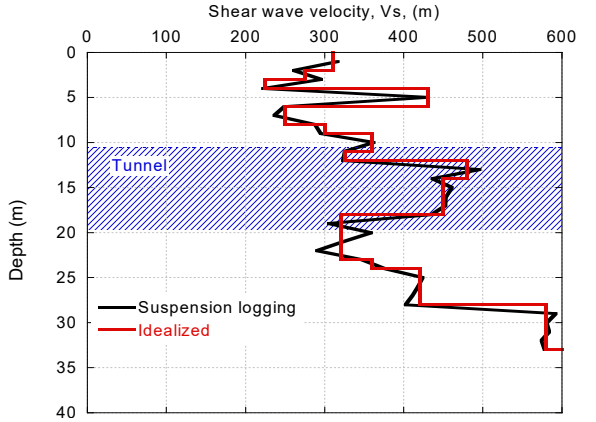

Figure 10. Shear wave velocity profile. Vs average=370m/s, Vs30=358m/s

5 SEISMIC SOIL–TUNNEL–BUILDING INTERACTION

Figures 11, 12 and 13 summarize the PGA recorded at the near field, free field and foundation for all components, during the earthquakes compiled in Table 1. The orientation of the accelerometers located in the building (i.e. control points C and D) differs from the orientation of those placed outside the building (i.e. control points A and B). Thus, it was necessary to project these recordings to ensure the same orientation, to be able to analyze the seismic interaction of the tunnel–soil–building system. The kinematic soil-building interaction is considered beneficial because it attenuates motion associated with the embedding effect (due to the foundation depth) and a motion uniformity effect due to the kinematic constraint of the foundation slab. The embedding effect can be estimated using Equation 1 proposed by Kausel et al. (1978). While the uniformization effect of the movement by rigid foundation with equation 2 (adapted from Veletsos and Prasad, 1989).

$$H_c = \begin{cases} \cos\left(\frac{\pi}{2} * \frac{\omega}{\omega_c}\right) & if\ \omega \le 0.7\omega_c \\ 0.453 & if\ \omega > 0.7\omega_c \end{cases} \quad (1)$$

$$\omega_c = \pi V_{sf}/2d$$

$$H_u(\omega) = \left\{\frac{1}{b_o^2}[1 - exp(-2b_0^2)(M)]\right\}^{\frac{1}{2}} \quad (2)$$

$$M = \begin{cases} 1 + b_0^2 + b_0^4 + \frac{b_0^6}{2} + \frac{b_0^8}{4} + \frac{b_0^{10}}{12}; & for \quad b_0 \le 1 \\ \exp(2b_0^2)\left[\frac{1}{\sqrt{\pi}b_0}\left(1 - \frac{1}{16b_0^2}\right)\right]; & for\ b_0 > 1 \end{cases}$$

$$b_0 = 0.00065 * \omega \sqrt{A/\pi}$$

where, $\omega = f * 2\pi$, is the circular frequency of the excitation; d is the embedment depth, V_{sf} is the shear wave velocity below the foundation, A is the area of the foundation footprint.

As can be seen, the equations are a function of the excitation frequency. Considering that local earthquakes concentrate their energy at high frequencies (10-50 Hz), both H_c and H_u transfer functions were calculated using the following values: *f = 30 Hz (average between 10 and 50 Hz)*, *Vsf = 280 m/s*, *d = 1.5 m*, and *A = 200 m²*. With these values, H_c=0.9 and H_u=0.70 were obtained. Thus, overall, it would be expected that the movement in the foundation would be 0.63 of the movement in the free field. Regarding the results from the seismic records, this reduction called in here "efficiency factor due to the foundation", EF_f, defined as the ratio between the PGA at foundation and near field, PGA_f/PGA_{nf}, ranges from 0.74 to 0.08, and has an average value of 0.22. The reported EF_f values

indicate that the foundation is efficient in reducing the seismic movement and the amplification effects of the tunnel, due to these occur in high frequencies. Interestingly, the foundation exhibits lower PGA values than those recorded in the free field, which highlights the importance of implementing a resistant stiff foundation, even in competent soils. Therefore, those structures with non-engineering foundations could have structural damage due to the presence of the tunnel. Likewise, the level of particle velocity, in some of these earthquakes has reached values close to the limits proposed by the DIN 4150 and SS 640 regulations (Figure 14), which could damage nearby structures during earthquakes of greater magnitude and considering that local earthquakes usually occur in series of continuous events (swarms), this aspect becomes more relevant.

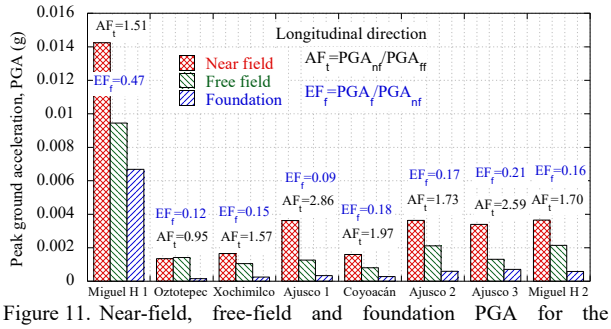

Figure 11. Near-field, free-field and foundation PGA for the longitudinal direction.

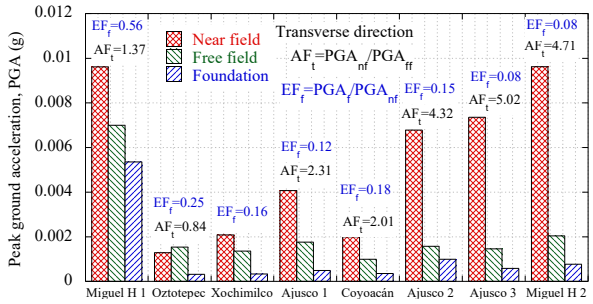

Figure 12. Near-field and free-field and foundation PGA for the transverse direction.

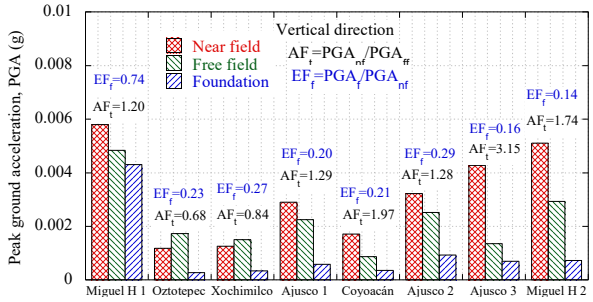

Figure 13. Near-field and free-field and foundation PGA for the vertical direction.

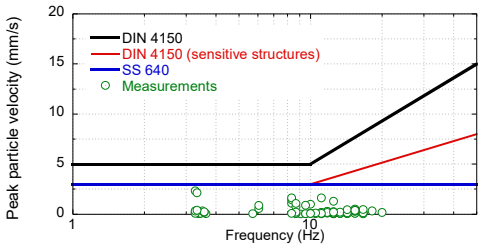

Figure 14. Comparison of the measured vibrations with limiting values established by international normativism.

Figures 15, 16 and 17 present the comparison of the response spectra obtained for the records in the free field, the near field and the foundation, which are normalized by their corresponding PGA. The response spectra shows that the foundation responds to periods greater than the free field or the near field since the building has a fundamental period of Te= 0.28s (fe=3.6Hz), far from that of the movements recorded in the free field and near field, which can explain the peak in periods of around 0.3 s that can be observed in the spectra of the horizontal components (longitudinal and transverse). A similar, tough less pronounced, effect is observed in the vertical component in shorter periods (0.15s).

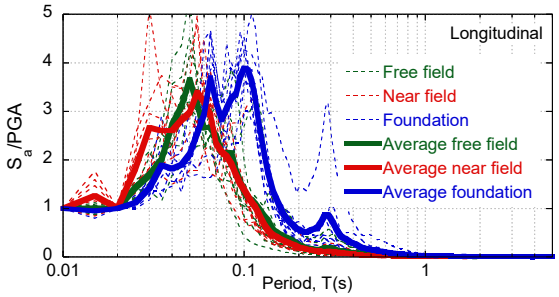

Figure 15. Response spectra normalized of the longitudinal direction.

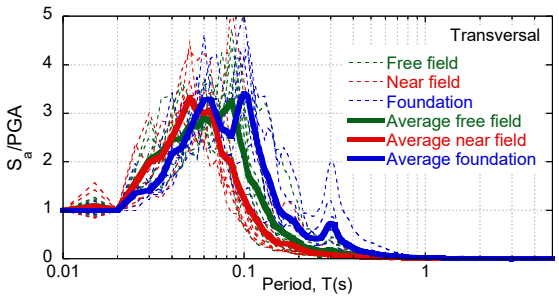

Figure 16. Response spectra normalized of the transversal direction.

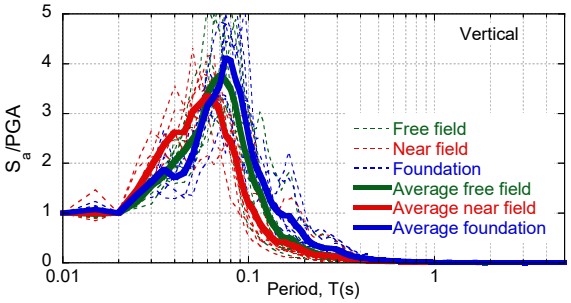

Figure 17. Response spectra normalized of the vertical direction.

Figures 18, 19 and 20 depict the empirical transfer functions between near field and free field. The presence of the tunnel amplifies the free-field motion for the entire frequency range in all three components, and although there are intervals of attenuation for each earthquake, these are not observed in the general trend (i.e., the average). Based on the trend lines, it was possible to identify that the vertical component has a greater amplification starting at frequencies greater than 12 Hz, while for the longitudinal and transverse components this increase occurs since 3.8 and 3.5 Hz, respectively. Previous studies (Rabeti Moghadam & Baziar, 2016; Yiouta-Mitra et al., 2007) suggest that the tunnel effect on the surface seismic response increases as the wavelength of the ground motion gets closer to the tunnel dimensions. Basically, this issue can be associated partially with the dispersion and wave-scattering effect of the short waves, which corresponds to the high-frequency seismic motion component, where the local earthquakes concentrate most of their energy.

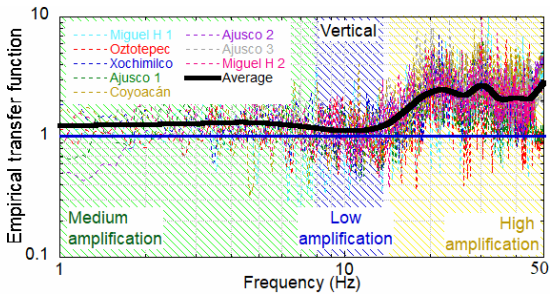

Figure 18. Empirical transfer functions between near field and free field for longitudinal component.

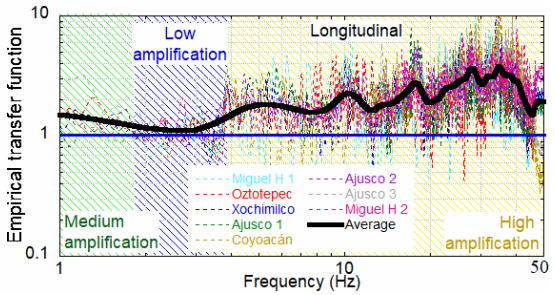

Figure 19. Empirical transfer functions between near field and free field for transverse component.

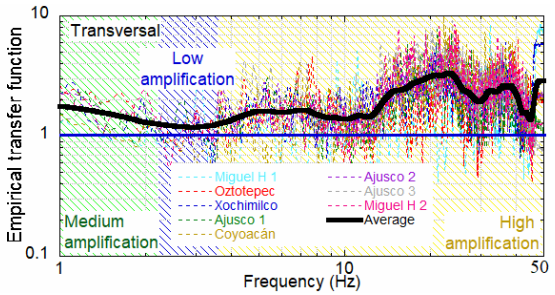

Figure 20. Empirical transfer functions between near field and free field for vertical component.

Figures 21, 22 and 23 show the empirical transfer functions between foundation and free field. As can be observed, the foundation has almost the same movement in the horizontal components than the free field for all frequencies lower than 2 Hz, from which the amplitude grows, until reaching a maximum value in a frequency range between 3 to 4 Hz. The frequencies at which this peak value is reached can be related to the fundamental frequency of the building (3.6Hz). Once this peak is reached the movement is attenuated and moves to a stable zone with values around 1, where the behavior is random. For the horizontal components, and especially in the longitudinal one, another frequency range with amplification is presented (between 7 and 11 Hz). Once this range is exceeded the amplitude of the movement in the foundation is less than that of the free field, showing high attenuation for frequencies larger than 10 Hz. On the other hand, for the vertical component, after reaching the stable zone (4 and 8 Hz) the movement is attenuated for the rest of the frequencies. Figures 24, 25 and 26 present the transfer functions between the roof and the foundation. As can be seen, for the horizontal components, the largest amplification of motion occurs in the ranges where the previous transfer functions (i.e., foundation/free field) present the maximum values (i.e. from 3 to 4 Hz and 8 to 9 Hz). After this maximum, the value drops to 1 for a frequency of around 8 Hz, then its behavior becomes more erratic up to 25 Hz, from where a decrease in movement is observed (i.e. values less than 1). On the other hand, the vertical component is amplified at both high and low frequencies and presents a frequency range in which the motion is not modified (between 2 and 5 Hz).

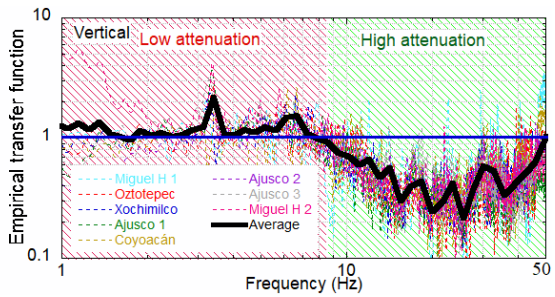

Figure 21. Empirical transfer functions between foundation and free field for longitudinal component.

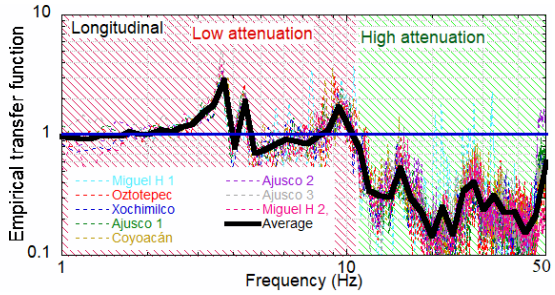

Figure 22. Empirical transfer functions between foundation and free field for transverse component.

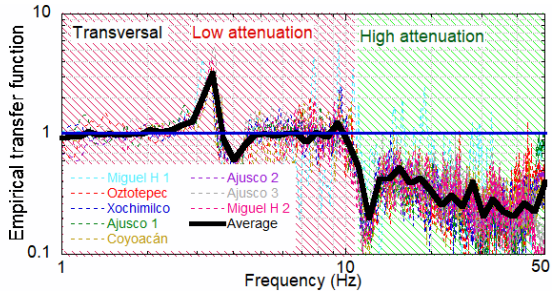

Figure 23. Empirical transfer functions between foundation and free field for vertical component.

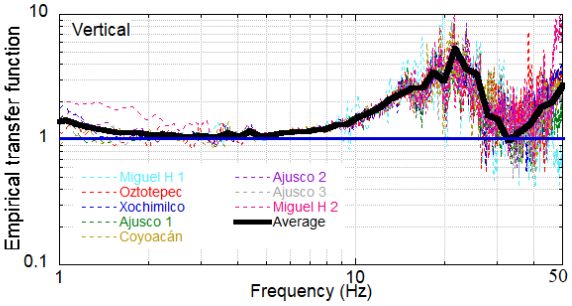

Figure 24. Empirical transfer functions between building roof and foundation for longitudinal component.

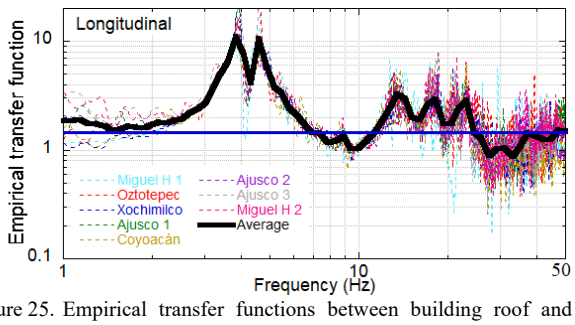

Figure 25. Empirical transfer functions between building roof and foundation for transverse component.

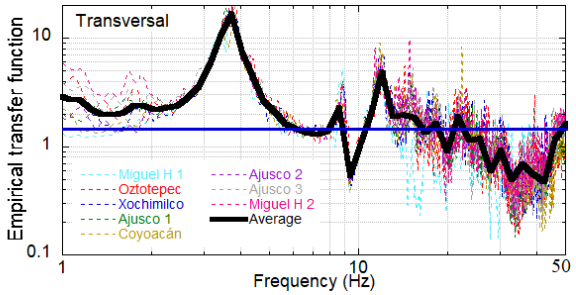

Figure 26. Empirical transfer functions between building roof and foundation for vertical component.

6 CONCLUSIONS

This paper presents the results gathered from the seismic instrumentation of a tunnel–soil–building test site in Mexico City during eight local earthquakes. An arrangement of four accelerometers was deployed at the site, to establish the seismic response of the free field, near field, and the building. It was concluded that even in low-to medium-magnitude events, the presence of the tunnel leads to PGA amplification both in the horizontal and in the vertical components, ground motion incoherence, and spectral accelerations amplification, especially at high frequencies. From all the records of the local earthquakes in the near field, it was found that 88% presents a PGA amplification in comparison to the accelerations in free field, associated with the interaction effect of the tunnel, with a maximum value of 4.4 and an average of 2.

Comparisons among local, intraplate, and interface earthquakes reveal that tunnel interaction effects are strongly frequency dependent. Notably, differences in Fourier amplitudes between near field and free field, become increasingly prominent as the energy of the earthquake concentrates in high frequencies. This behavior can be partially attributed to dispersion and wave-scattering effects of the short waves, which begin to be noted when the wavelengths are comparable to the tunnel dimensions.

Regarding the impact of the tunnel effect on the building behavior, it was observed that its foundation is capable of attenuate the tunnel's effect over a wide range of frequencies. According to the EF_f values defined by the high frequency range (10 to 50Hz), the foundation reduced on average the 78% of the Fourier amplitude of the ground motion of near field. This highlights the importance of kinematic effect of the rigid foundation slab, which can reduce the translation response.

It is important to note that structures with more flexible foundations could be more susceptible to the incoherent ground motion generated by the tunnel, and rigid structures with short fundamental period of vibrations (<0.1 s). Therefore, research on this topic is critical to advance seismic design practices.

Finally, it is important to highlight that the findings are derived from relatively low magnitude events (<M2.1) recorded during almost 1 year of monitoring. Although the tunnel-building interaction effects were clearly captured from the seismic records, more seismic records should be analyzed before generalizing the findings. Therefore, the implemented instrumentation will continue monitoring to expand the database (magnitude, distance and types of earthquakes), seeking to improve the findings presented in here.

7 REFERENCES

Abrahamson, N.A., Schneider, J.F., and Stepp J.C. 1991. Empirical Spatial Coherency Functions for Application to Soil-Structure Interaction Analyses. *Earthquake Spectra* 1991; 7 (1): 1–27.

Baziar, M.H., Moghadam, M.R., Kim, D.S., and Choo, Y.W. 2014. Effect of underground tunnel on the ground surface acceleration. *Tunnelling and Underground Space Technology* 44: 10–22.

Davies, R., Foulger, G., Bindley, A., and Styles, P. 2013. Induced seismicity and hydraulic fracturing for the recovery of hydrocarbons. *Mar Petrol Geol*, 45, pp. 171-185.

European Comittee for Standardization, 1986. *DIN-4150 Structural vibrations in buildings. Deutsches Institut fur Normung Berlin*

Frohlich, C., Hayward, C., Stump, B., and Potter, E. 2011 The Dallas–Fort Worth Earthquake Sequence: October 2008 through May 2009. *Bulletin of the Seismological Society of America*; 101 (1)

Hashash, Y., Dashti, S., Musgrove, M., Gillis, K., Walker, M., Ellison, K., and Basarah, Y. 2018. Influence of tall buildings on seismic response of shallow underground structures. *Journal of Geotechnical and Geoenvironmental Engineering* 144(12).

Jaimes, M.A., and Suárez, G. 2025. Estimation of Damage Scenarios in the Mexico City Basin Caused by Local Crustal Earthquakes. *Bulletin of the Seismological Society of America*.

Kausel, E., Whitman, R.V., Morray, J.P., and Elsabee, F. 1978 The spring method for embedded foundations, *Nuclear Engineering and Design,* Vol. 48, 1978.

Mayoral, J.M., De La Rosa, D., Alcaraz, M., and Barragan, E. 2023. Tunnel-soil-bridge seismic interaction on soft clay. *Soil Dynamics and Earthquake Engineering*, 164.

Mayoral, J.M., and Mosqueda, G. 2020. Seismic interaction of tunnel-building systems on soft clay. *Soil Dynamics and Earthquake Engineering*, 139(September), 106419.

Mayoral, J.M. and Mosqueda, G. (2021). Foundation enhancement for reducing tunnel-building seismic interaction on soft clay. *Tunnelling and Underground Space Technology* 115, 104016.

Mayoral, J.M., Alcaraz, B., and Tepalcapa, S. 2023. Seismic performance of soil–tunnel–building systems in stiff soils. *Earthquake Spectra* 2023, Vol. 39(2) 1214–1239.

Mayoral, J.M., Pérez, M., Román-de la Sancha, A., and Rosas, J. 2025. Seismic Performance of Modal Transfer Stations on Soft Clays. *Applied Sciences*, 15(6), 3406.

Moghadam, M.R., and Baziar, M.H. 2016. Seismic ground motion amplification pattern induced by a subway tunnel: Shaking table testing and numerical simulation. *Soil Dynamics and Earthquake Engineering* 83 (2016)81–97.

Pitilakis, K., Tsinidis, G., Leanza, A. and Maugeri, M. 2014. Seismic behaviour of circular tunnels accounting for above ground structures interaction effects. *Soil Dynamics and Earthquake Engineering* 67: 1–15.

Rabeti Moghadam, M., & Baziar, M. H. 2016. Seismic ground motion amplification pattern induced by a subway tunnel: Shaking table testing and numerical simulation. *Soil Dynamics and Earthquake Engineering*, 83, 81–97.

Schweizerische Normen-Vereinigung, 1992. *SN 640 312a-1992. Lesébranlements – Efeet des ebranlements sur les construction, Zürich (in Swiss)*

Van, E., Mulders, F., Nepveu, M., Kenter, C.J., and Scheffers, B. 2006. Correlation between hydrocarbon reservoir properties and induced seismicity in the Netherlands. *Engineering Geology* Volume 84, Issues 3–4, 16 May 2006, Pages 99-111.

Veletsos, A., and Prasad, A.M. 1989. Seismic Interaction of Structures and Soils: Stochastic Approach. *Journal of Structural Engineering* Volume 115, Issue 4 April 1989

Wang, G., Yuan, M., Yu, M., Wu, J., and Wang, Y. 2018. Experimental study on seismic response of underground tunnel-soil-surface structure interaction system. *Tunnelling and Underground Space Technology* 76 (2018) 145–159.

Yiouta-Mitra, P., Kouretzis, G., Bouckovalas, G., and Sofianos, A. 2007. Effect of underground structures in earthquake resistant design of surface structures.

Zuñiga, F.R., and Suarez, G. 2017. *A first-order seismotectonic regionalization of Mexico for seismic hazard and risk estimation.* Journal of Seismology 21: 1295–1322.